Chapter 1

Quantum Cascade Laser Design and Operation Theory

To innovate in QC laser structures and designs, a solid understanding of their operation is absolutely essential. In this chapter, I lay out the basic tools and derive the fundamental relations important to QC laser design and operation. This theory becomes the foundation for ideas for and understanding derived from new designs presented in later chapters. Rarely does one find a thorough survey of QC laser theory collected in one place. I hope to accomplish this in this chapter.

1.1 The Schrödinger Equation

Fundamental to QC laser design is the the ability to accurately calculate the positions of energy states in the quantum-confined dimension. In the elementary abstraction, we simply solve the time-independent Schrödinger equation

$$-\frac{\hbar^2}{2m^*}\frac{\partial^2}{\partial z^2}\psi(z) + V(z)\psi(z) = \mathcal{E}\psi(z) \tag{1.1}$$

where $\hbar$ is Planck's constant, m^* is the electron effective mass, z is the dimension of quantum confinement, ψ is the electron wavefunction, V is the quantum well potential energy, and $\mathcal{E}$ is the eigen energy of the quantum state.

Right away, we run into a problem. The effective mass in semiconductors is energy-dependent: as the electron acquires more energy—gets higher up in the band and closer

to the vacuum level—the electron gets heavier. Also, our QC structure is a system of layered materials, each with a different effective mass from adjacent layers. So, the effective mass is both energy- and position-dependent: $m^*(z,\mathcal{E})$. This results in a small change to the standard Schrödinger equation. When solving the Schrödinger equation, we are taught to match $\psi(z)$ and $\frac{\partial}{\partial_z}\psi(z)$ at the boundaries. Now, with variable effective masses, the solutions of envelope functions [cite: Harrison p. 36] are continuous across material interfaces in both $\psi(z)$ and $\frac{1}{m^*}\frac{\partial}{\partial z}\psi(z)$.

Because of variable effective mass, the classical portrayal of the Schrodinger equation is somewhat different. Given the momentum operator $\mathcal{P}_z = -i\hbar\partial_z$, the kinetic energy operator becomes

$$\mathcal{T} = \mathcal{P}_z \frac{1}{m^*(z,\mathcal{E})}\mathcal{P}_z = -\frac{\hbar^2}{2}\frac{\partial}{\partial z}\frac{1}{m^*(z,\mathcal{E})}\frac{\partial}{\partial z} \tag{1.2}$$

and the Schrodinger equation now becomes

$$-\frac{\hbar^2}{2}\frac{\partial}{\partial z}\frac{1}{m^*(z,\mathcal{E})}\frac{\partial}{\partial z}\psi(z) + V(z)\psi(z) = \mathcal{E}\psi(z) \tag{1.3}$$

Now, to make this a discreet equation, we approzimate the derivative as

$$\frac{\mathrm{d}f}{\mathrm{d}z} \approx \frac{\Delta f}{\Delta z} = \frac{f(z+\delta z) - f(z-\delta z)}{2\delta z}\,. \tag{1.4}$$

The Schrodinger equation above can be discretized by ezpanding $\mathcal{T}\psi(z)$.

$$\frac{\frac{1}{m^*(z+\delta z,\mathcal{E})}\frac{\partial\psi(z)}{\partial z}\Big|_{z+\delta z} - \frac{1}{m^*(z-\delta z,\mathcal{E})}\frac{\partial\psi(z)}{\partial z}\Big|_{z-\delta z}}{2\delta z} = \frac{2}{\hbar^2}[V(z)-\mathcal{E}]\psi(z) \tag{1.5}$$

Applying Eq. (1.4) to the above equation, gathering terms in $\psi(z)$, and making the transformation $2\delta z \to \delta z$ gives

$$\begin{aligned}\psi(z+\delta z) = \Bigg\{\Bigg[\frac{2(\delta z)^2}{\hbar^2}[V(z)-\mathcal{E}] + \frac{1}{m^*(z+\delta z/2,\mathcal{E})} + \frac{1}{m^*(z-\delta z/2,\mathcal{E})}\Bigg]\psi(z) \\ - \frac{1}{m^*(z-\delta z/2,\mathcal{E})}\psi(z-\delta z)\Bigg\} m^*(z+\delta z/2,\mathcal{E})\end{aligned} \tag{1.6}$$

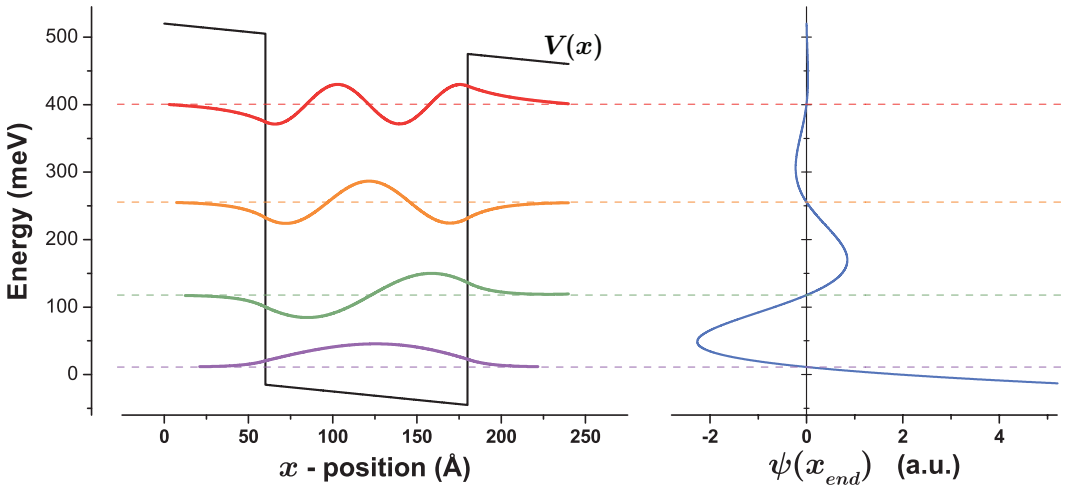

Figure 1.1: Example use of the shooting method. The left panel shows a potential $V(z)$ for an $In_{0.53}Ga_{0.47}As$ / $Al_{0.48}In_{0.52}As$ quantum well with $E_{field} = 25$ kV/cm. Four bound solutions are found by finding the roots of $\psi(z_{end})$, as shown in the right panel. The wavefunction $\psi(z)$ is plotted for the four bound solutions.

The effective mass at the intermediate points $z \pm \delta z/2$ is found by taking the average of the effective mass for the two adjacent points z and $z + \delta z$.

The shooting method is used to solve for the eigen energies of our system through the application of Eq. (1.6). Specifically, we look for bound solutions of the system; that is, any energy $\mathcal{E}$ where $\psi(0) = 0$ and $\psi(z_{end}) = 0$. In an elementary implementation of the shooting method, the energy space covered by our potential $V(z)$ is initially divided into many discreet steps. Using the initial conditions $\psi(0) = 0$ and $\psi(1) = 1$, Eq. (1.6) is used to propagate through discreet steps in z to find $\psi(z_{end})$ for each initial energy value. To find the ezact energy value of a bound solution, we take advantage of the fact that $\psi(z_{end})$ switches signs at a bound solution. Therefore, when $\psi(z_{end})$ is plotted for all energies over our energy space, noting the location in energy of a sign flip of $\psi(z_{end})$, allows us to iterate in energy around this point to find the ezact value of the bound solution. Figure 1.1 provides an ezample; here, our potential $V(z)$ is for a single quantum well in the $In_{0.53}Ga_{0.47}As$ / $Al_{0.48}In_{0.52}As$ system, with conduction band offset of 520 meV, and an applied electric field $E_{field} = 25$ kV/cm. Four bound solutions are found, and $\psi(z)$ is plotted for each solution, using the eigen energy as the baseline of the wavefunction.

1.2 Semiconductor Interface Energy Offsets and Band Gaps

To properly use Eq. (1.6) solving the time-independent Schrödinger equation, we need accurate knowledge of two key parameters: $V(z)$ and $m^*(z,\mathcal{E})$. This section is devoted to attaining the band offset values that are so important to coupled quantum well systems such as QC lasers. In the following section, we discuss effective mass in semiconductor systems. This section and the remaining sections in this chapter make heavy use of parameters for semiconductor materials; a superb review of important III–V materials parameters was published by Vurgaftman *et al.* in 2001 [1].

All QC laser implementations to date have used intersubband transitions in the conduction band. While QC electroluminescence has been shown from valence intersubband transitions [2] [3], we our more keenly interested in the conduction band edge offsets of materials. As it turns out, the valence band offsets have been much more extensively studied [1], owing to the experimental difficulty of measuring conduction band offsets. When reporting a valence band offset, the convention is to set a reference material with $VBO = 0$, and report all offsets relative to that material; Vurgaftman *et al.*, for example, define $VBO(\text{InSb}) = 0$. In this way, the valence band offset for any arbitrary two materials is easily found as the difference in VBO for the two materials of the set. By adding the bandgap of each material to its respective VBO, the conduction band offset for a two material system can likewise be calculated. More concretely, the conduction band edge (at the Γ point) $\mathcal{E}_c^\Gamma$ can be defined as

$$\mathcal{E}_c^\Gamma = VBO + \mathcal{E}_g^\Gamma + \delta\mathcal{E}_{Varsh} + \delta\mathcal{E}_{\varepsilon c} + \delta\mathcal{E}_{\varepsilon v} \tag{1.7}$$

where $\mathcal{E}_g^\Gamma$ is the energy gap at the Γ point at $T = 0$ K without strain, $\delta\mathcal{E}_{Varsh}$ is the Varshney correction to the bandgap energy for $T \neq 0$ K, and $\delta\mathcal{E}_{\varepsilon c}$ and $\delta\mathcal{E}_{\varepsilon v}$ are corrections to the conduction and valence band edges due to hydrostatic deformation (i.e. strain). Each of these terms is treated in the following sections. With this definition of $\mathcal{E}_c^\Gamma$, the conduction band offset at the interface between two materials A and B is $\mathcal{E}_c^\Gamma(A) - \mathcal{E}_c^\Gamma(B)$.

1.2.1 Materials parameters for ternary alloys

Fundamental materials parameters, VBO and $\mathcal{E}_g^\Gamma$ for example, can be conveniently reported in tabular form for binary semiconductors, as in the review by Vurgaftman *et al.* [1]. Ternary alloys, however, have a degree of freedom in material composition, making tabular recording prohibitive. For any ternary material $A_xB_{1-x}C$, composed proportionally of the two constituent binaries $(AC)_x$ and $(BC)_{1-x}$, a range of values exists over the mole fraction x for any arbitrary material parameter G. Conveniently, we can make use of the composition endpoints $x = 0$ and $x = 1$ to bound the possible values of G. Then, G can thus be defined as

$$G(A_xB_{1-x}C) = xG(AC) + (1-x)G(BC) + x(1-x)C_B \tag{1.8}$$

where C_B is the "bowing parameter" specific to material ABC. Commonly, the bowing parameter is either not well known, or no bowing parameter exists. In this case, the material parameter is just a linear interpolation between the value of the parameter for the two component binaries weighted by x.

1.2.2 Temperature effects on bandgap

The temperature dependence of semiconductor bandgaps is commonly described with the Varshni formula. This is an empirical formula that fits two Varshni parameters—α $[\frac{\text{energy}}{\text{temperature}}]$ and β [temperature]—to experimentally obtained values of bandgap with temperature. The Varshni formula gives the temperature T dependence of the bandgap as

$$\mathcal{E}_g(T) = \mathcal{E}_g(T=0) - \frac{\alpha T^2}{T+\beta} \tag{1.9}$$

so that the temperature correction to the conduction band edge is

$$\delta\mathcal{E}_{Varsh} = -\frac{\alpha T^2}{T+\beta}\,. \tag{1.10}$$

1.2.3 Strain effects on bandgap and band offset

Strain in epitaxially-grown semiconductors arises when the lattice constant for a particular composition of grown material is different from that of the substrate material. Generally, strain is an undesired condition, as strain buildup will eventually lead to a variety of epitaxial defects. The lattice constant and bandgap are both functions of the mole fraction x for any particular ternary material composition; therefore, imposing the condition that all grown materials are lattice-matched to the substrate lattice constant does not allow one to adjust mole fraction compositions to alter the material bandgap.

Since QC lasers operate on intersubband transitions, any optical transition must be confined within the quantum wells of the heterostructure to prevent electrons from escaping. It is thus easy to see that the ability to adjust material compositions to maximize the conduction band offset would be advantageous. This is especially true when seeking high energy, short wavelength photon generation.

The QC concept allows for a clever way to achieve both strain-free bulk material while simultaneously having the ability to adjust material compositions to affect bandgaps. Taking advantage of the alternating layer structure, where a wide bandgap barrier material is interleaved with a narrow bandgap well material, compressive strain can be built into one layer set while tensile strain is built into the other layer set; the result can be an overall strain-balanced heterostructure.

Semiconductors with a zinc blende lattice structure (cubic symmetry)—the case for most III–V alloys—acquire biaxial strain when epitaxially grown on a substrate with a different lattice constant. That means, for the three dimensional strain tensor, only the diagonal components ε_{xx}, ε_{yy}, and ε_{zz} are non-zero. Identifying z as the direction of epitaxial growth, values for strain are given by [4]

$$\varepsilon_{xx} = \varepsilon_{yy} = \frac{a_0 - a_{\ell c}}{a_{\ell c}} \tag{1.11a}$$

$$\varepsilon_{zz} = -\frac{2c_{12}}{c_{11}}\varepsilon xx \tag{1.11b}$$

where a_0 is the lattice constant of the substrate, $a_{\ell c}$ is the lattice constant of the epitaxial layer material, and c_{11} and c_{12} are the elastic stiffness constants of the layer material.

The effects of strain on bandgaps are well described by the Pikus–Bir interaction [5] and also be the "model-solid" theory of Van de Walle [6]. Here, the change in band gap

due to strain is empirically characterized by the relative change in volume due to strain and scaled by a hydrostatic deformation potential a [energy]. The change in volume due to strain is given by

$$\frac{\delta V}{V} = \varepsilon_{xx} + \varepsilon_{yy} + \varepsilon_{zz} \tag{1.12}$$

which is the trace of the strain tensor. The change in bandgap due to strain $\delta\mathcal{E}_\varepsilon$ is the

$$\delta\mathcal{E}_\varepsilon = a\frac{\delta V}{V} \tag{1.13}$$

and the components of the shift acquired by the conduction and valence bands, $\delta\mathcal{E}_{\varepsilon c}$ and $\delta\mathcal{E}_{\varepsilon v}$ respectively, are

$$\delta\mathcal{E}_{\varepsilon c} = a_c\frac{\delta V}{V} \tag{1.14a}$$

$$\delta\mathcal{E}_{\varepsilon v} = a_v\frac{\delta V}{V} \tag{1.14b}$$

where a_c and a_v are the conduction and valence band hydrostatic deformation potentials, given that $a = a_c + a_v$. In compound semiconductors, adding hydrostatic pressure (i.e. adding compressive strain) results in an increase in band gap. Generally, this means that compressive strain causes the conduction band edge to move "up" proportionally by $\frac{a_c}{a}$ and the valence band edge to move "down" proportionally by $\frac{a_v}{a}$.

The light hole (LH), heavy hole (HH), and split-off (SO) valence bands have p state "shape" and therefore lack spherical symmetry, unlike the conduction band (C) with s state shape. Due to this lack of symmetry, biaxial strain has a shear component that affects the valence bands, and it splits the degeneracy of the heavy hole and light hole bands at the Γ point. Derived from the Pikus–Bir Hamiltonian [5], the energy bandgaps with shear strain and including the spin-orbit interaction are

$$\mathcal{E}^\Gamma_{\text{C}-\text{HH}} = \mathcal{E}^\Gamma_g + \delta\mathcal{E}_{\varepsilon c} + \delta\mathcal{E}_{\varepsilon v} - Q_\varepsilon \tag{1.15a}$$

$$\mathcal{E}^\Gamma_{\text{C}-\text{LH}} = \mathcal{E}^\Gamma_g + \delta\mathcal{E}_{\varepsilon c} + \delta\mathcal{E}_{\varepsilon v} + \frac{1}{2}\left(Q_\varepsilon - \Delta_{\text{SO}} + \sqrt{\Delta^2_{\text{SO}} + 2\Delta_{\text{SO}}Q_\varepsilon + 9Q^2_\varepsilon}\right) \tag{1.15b}$$

$$\mathcal{E}^\Gamma_{\text{C}-\text{SO}} = \mathcal{E}^\Gamma_g + \delta\mathcal{E}_{\varepsilon c} + \delta\mathcal{E}_{\varepsilon v} + \frac{1}{2}\left(Q_\varepsilon - \Delta_{\text{SO}} - \sqrt{\Delta^2_{\text{SO}} + 2\Delta_{\text{SO}}Q_\varepsilon + 9Q^2_\varepsilon}\right) \tag{1.15c}$$

where Δ_{SO} is the split-off energy without strain and the shear deformation potential b [energy] is included in Q_ε, defined as

$$Q_\varepsilon = \frac{b}{2}\left(\varepsilon_{xx} + \varepsilon_{yy} - 2\varepsilon_{zz}\right) . \tag{1.16}$$

The bandgaps given in Eq. (1.15a) neglect temperature effects, which can be included by adding the $\delta\mathcal{E}_{Varsh}$ term.

1.3 Effective Mass

1.4 Self-consistent Solutions of the Schrödinger and Poisson Equations

Knowing the energy gaps and band offsets of our materials system, we can calculate the semiconductor material potential profile $V_{mat}(z)$. However, when semiconductors are doped, the fixed and free charges (ionized impurities and free electrons) that make up a charge distribution ρ add a perturbation to the potential profile. Given by the Poisson equation, this perturbation V_ρ is

$$\nabla^2 V_\rho = -\frac{\rho}{\epsilon} \tag{1.17}$$

where $\epsilon = \epsilon_r \epsilon_0$ is the material permittivity. The potential $V_\rho(z)$ can otherwise be found through the electric field strength $E(z)$

$$V_\rho(z) = \int_{-\infty}^{z} E(z)\, dz . \tag{1.18}$$

With our system of energy states quantized in one dimension (z), and our wavefunctions $\psi(z)$ numerically solved at discreet points with spacing δz, we can think of the charge density $\rho(z)$ as infinite sheets, with sheet density $\sigma(z)$ and thickness δz. The resultant perpendicular electric field to an infinite plane of charge is

$$E = \frac{\sigma}{2\epsilon} \tag{1.19}$$

and we can thus sum the contributions to the aggregate electric field from all of the individual "slices" of δz as

$$E(z) = -\sum_{z'=-\infty}^{z-\delta z} \frac{\sigma(z')}{2\epsilon} + \sum_{z'=z}^{\infty} \frac{\sigma(z')}{2\epsilon} \tag{1.20}$$

which accounts for the sign of the field being dependent on the location of the position z relative to the position of the charge slice z'. The sheet charge density $\sigma(z)$ includes both negative free electron charge and positive ionized impurity charge. For a doping density profile $N_d(z)$ $[\frac{1}{\text{volume}}]$, the total free electron sheet density n_s $[\frac{1}{\text{area}}]$ will be given by

$$n_s = \int_{-\infty}^{+\infty} N_d(z)\, dz \tag{1.21}$$

and the fixed charge sheet density is $N_d(z)\delta z$. The net sheet charge density is thus

$$\sigma(z) = q\left[N_d(z)\delta z - n_s \psi_i^*(z)\psi_i(z)\right] \tag{1.22}$$

where q is the absolute value of the electron charge ($q = |q|$) and if all free electrons are in the quantum state i. If all electrons are not in a single quantum state (i.e. $T \neq 0$ K), we can distribute them over the set of relevant states using the Fermi distribution. For the quantum state i at energy $\mathcal{E}_i$, the Fermi distribution is

$$f(\mathcal{E}_i) = \frac{1}{e^{\frac{\mathcal{E}_i - \mathcal{E}_f(T)}{k_B T}}} \tag{1.23}$$

where $\mathcal{E}_f(T)$ is the Fermi energy at temperature T given by

$$\mathcal{E}_f(T) = k_B T \ln\left(e^{\frac{\mathcal{E}_f(0)}{k_B T}} - 1\right) \tag{1.24}$$

and

$$\mathcal{E}_f(0) = n_s \frac{\pi\hbar^2}{m^*\epsilon_0}\,. \tag{1.25}$$

Our sheet charge density now becomes

$$\sigma(z) = q\left[N_d(z)\delta z - \sum_{i=1}^{n} f(\mathcal{E}_i) n_s \psi_i^*(z)\psi_i(z)\right] \tag{1.26}$$

for the electron-occupied set of quantum states $1:n$. Ensure $\sum_{i=1}^{n} f(\mathcal{E}_i) n_s = n_s$.

Following the above procedure to find the charge potential V_ρ, we can apply this correction as a perturbation to the overall potential: $V(z) = V_{mat}(z) + V_\rho(z)$. We can then solve our system using Eq. (1.6) and the shooting method described previously with new composite potential. Certainly, the perturbation from V_ρ changes the solution to the system enough that a new V_ρ can be calculated based on the shifted electron wavefunctions. Thus, an iterative approach is needed, where V_ρ is updated after each iteration until consecutive solutions converge.

1.5 Optical Dipole Matrix Element

1.6 LO-phonon Scattering Time

1.7 Optical Gain

1.8 Figure of Merit and Modal Gain

1.9 Forms of Optical Loss

1.10 Threshold Current

Material gain γ $[\frac{1}{\text{length}}]$ is defined such that mode intensity $\mathcal{I}$ after some distance L is given by

$$\mathcal{I}(L) = \mathcal{I}(0) e^{\gamma L} \tag{1.27}$$

and

$$\gamma = \begin{matrix}\text{gain region} \\ \text{overlap with} \\ \text{optical mode}\end{matrix} \times \begin{matrix}\text{“strength” of the} \\ \text{gain material}\end{matrix} \times \begin{matrix}\text{population} \\ \text{inversion}\end{matrix} = \Gamma \sigma_0 (N_u - N_\ell) \tag{1.28}$$

where $(N_u - N_\ell)$ $[\frac{1}{\text{volume}}]$ represents the population inversion density between the upper u and lower ℓ states of the optical transition. The transition (gain) cross-section at peak

gain σ_0 [area] for the mode photon energy $\mathcal{E}_{ph}$ is

$$\sigma_0 = \frac{4\pi q^2}{hc\epsilon_0 n_{eff}} \frac{\mathcal{E}_{ph}}{\delta\mathcal{E}_{u\ell}} z_{u\ell}^2 \tag{1.29}$$

and the one-dimensional confinement factor Γ is defined as

$$\Gamma = \frac{\int_{x_0}^{x_0+d_{ac}} n(x) f^2(x)\, dx}{\int_{-\infty}^{\infty} n(x) f^2(x)\, dx} \tag{1.30}$$

where x_0 marks the beginning of the active core, d_{ac} is the thickness of the active core, $n(x)$ is the refractive index profile, and $f(x)$ is the electric field profile of the mode normalized such that $\max(f(x)) = 1$. The confinement factor can be further simplified by defining $d_m = \int_{-\infty}^{\infty} n(x) f^2(x)\, dx$ as the effective thickness of the optical mode.

A QC laser adds the complication of multiple periods of the active–injector region structure cascaded together into a single active core. In a general sense, each individual QC period i may have its own unique properties. Aggregate properties for the whole of the QC structure are given by summing over the individual QC periods.

$$\gamma = \sum_{i=1}^{N_p} \Gamma_i \sigma_{0,i} (N_{u,i} - N_{\ell,i}) \tag{1.31}$$

where Γ_i is now defined for an individual QC period as

$$\Gamma_i = \frac{\int_{x_i}^{x_i+d_{ap}} n(x) f^2(x)\, dx}{d_m} \tag{1.32}$$

with d_{ap} being the thickness of the QC active–injector period, so that summing over all d_{ap} yields d_{ac} and summing over all Γ_i yields the composite active core Γ.

Laser threshold is most easily derived assuming the gain clamping condition

$$\gamma = \alpha_{total} \tag{1.33}$$

with total optical loss α_{total} [$\frac{1}{\text{length}}$] being the sum of mirror loss α_m and waveguide loss α_w. Assuming each active period has the same transition cross-section and lifetime

profile, applying Eq. 5 to Eq. 7 yields

$$\alpha_m + \alpha_w = N_p \Gamma \sigma_0 (N_u - N_\ell)_{th} \tag{1.34}$$

where N_p results from summing over all active periods and the population density $(N_u - N_\ell)$ is at threshold. For a single QC period,

$$(N_{u,i} - N_{\ell,i})_{th} = \underset{\text{rate}}{\text{pumping}} \times \underset{\text{state lifetime}}{\text{effective upper}} = \frac{J_{th}}{q d_{ap,i}} \tau_{eff,i} \tag{1.35}$$

where τ_{eff} is the effective upper state lifetime. For the case of a two level system, $\tau_{eff} = \tau_u \left(1 - \frac{\tau_\ell}{\tau_{u\ell}}\right)$.

Now,

$$J_{th} = q \frac{\alpha_{total}}{\Gamma \frac{N_p}{d_{ac}} \sigma_0 \tau_{eff}} = \frac{hc\epsilon_0 n_{eff}}{4\pi q} \frac{\alpha_{total}}{\Gamma \frac{N_p}{d_{ac}} \frac{\mathcal{E}_{u\ell}}{\delta \mathcal{E}_{u\ell}} z_{u\ell}^2 \tau_{eff}} \tag{1.36}$$

1.11 Rate Equations for QC Lasers

Rate equations are a phenomenological method for describing laser devices from which important performance parameters (*e.g.* output power, wall-plug efficiency, threshold, etc.) can be derived. Describing the change with respect to time in the total upper state population $\mathcal{N}_u$, total lower state population $\mathcal{N}_\ell$, and total photon population $\mathcal{N}_{ph}$ of the system gives the system of equations,

$$\underset{\text{w.r.t. time}}{N_u \text{ change}} = \underset{\text{rate in}}{\text{non-radiative}} - \underset{\text{rate out}}{\text{non-radiative}} - \underset{\text{transition rate}}{\text{radiative}} \tag{1.37a}$$

$$\underset{\text{w.r.t. time}}{N_\ell \text{ change}} = \underset{\text{rate in}}{\text{non-radiative}} - \underset{\text{rate out}}{\text{non-radiative}} + \underset{\text{transition rate}}{\text{radiative}} \tag{1.37b}$$

$$\underset{\text{w.r.t. time}}{N_{ph} \text{ change}} = \underset{\text{transition rate}}{\text{radiative}} - \underset{\text{loss rate}}{\text{photon}} \tag{1.37c}$$

where non-radiative transition rates are given by the population of the state $\mathcal{N}_i$ divided by the non-radiative lifetime τ_i for the state i. Radiative transition rates are given by

$$\underset{\text{transition}}{\text{rate of radiative}} = \left(\underset{\text{for stimulated emission}}{\text{population available}} - \underset{\text{for absorption}}{\text{population available}} \right) \times \underset{\text{emission}}{\text{probability of stimulated}}$$

and

$$\begin{matrix}\text{probability of}\\ \text{stimulated}\\ \text{emission}\end{matrix} = \begin{matrix}\text{photon}\\ \text{density}\end{matrix} \times \begin{matrix}\text{photon}\\ \text{speed}\end{matrix} \times \begin{matrix}\text{transition}\\ \text{cross-section}\end{matrix}$$

In a semiconductor injection laser, the rate equations are expressed as

$$\frac{d\mathcal{N}_u}{dt} = \eta_{inj}\frac{I}{q} - \frac{\mathcal{N}_u}{\tau_u} - (\mathcal{N}_u - \mathcal{N}_\ell)\frac{\mathcal{N}_{ph}}{V_m}v_g\sigma_0 \tag{1.38a}$$

$$\frac{d\mathcal{N}_\ell}{dt} = \frac{\mathcal{N}_u}{\tau_{u\ell}} - \frac{\mathcal{N}_\ell}{\tau_\ell} + (\mathcal{N}_u - \mathcal{N}_\ell)\frac{\mathcal{N}_{ph}}{V_m}v_g\sigma_0 \tag{1.38b}$$

$$\frac{d\mathcal{N}_{ph}}{dt} = (\mathcal{N}_u - \mathcal{N}_\ell)\frac{\mathcal{N}_{ph}}{V_m}v_g\sigma_0 - \frac{\mathcal{N}_{ph}}{\tau_{ph}} \tag{1.38c}$$

where $\eta_{inj}\frac{I}{q}$ is the pumping rate for the upper laser state, V_m is the effective volume of the optical mode, and τ_{ph} is the photon lifetime in the cavity. The group velocity v_g is approximated by the phase velocity c_0/n_{eff}, which is accurate when dispersion low.

The traditional representation for rate equations with $N\left[\frac{1}{\text{volume}}\right]$ being the population density of the level is

$$\frac{dN_u}{dt} = \eta_{inj}\frac{I}{qV} - \frac{N_u}{\tau_u} - v_g\sigma_0(N_u - N_\ell)N_{ph} \tag{1.39a}$$

$$\frac{dN_\ell}{dt} = \frac{N_u}{\tau_{u\ell}} - \frac{N_\ell}{\tau_\ell} + v_g\sigma_0(N_u - N_\ell)N_{ph} \tag{1.39b}$$

$$\frac{dN_{ph}}{dt} = \Gamma v_g\sigma_0(N_u - N_\ell)N_{ph} - \frac{N_{ph}}{\tau_{ph}} \tag{1.39c}$$

Our strategy for applying these rate equations to QC lasers will again be to treat each active period individually. Thus, the rate equations will represent the populations associated with a single active period, and the final resultant parameters will be summed over all active periods. For QC lasers, it is convenient to work with energy level populations in terms of sheet density $n\left[\frac{1}{\text{area}}\right]$, which is the result when multiplying all equations by the gain region thickness d_{ap}; that is, since N is an electron density for a single QC

period, $n = N \times d_{ap}$.

$$\frac{dn_u}{dt} = \eta_{inj}\frac{I}{qV}d_{ap} - \frac{n_u}{\tau_u} - v_g\sigma_0(n_u - n_\ell)N_{ph} \tag{1.40a}$$

$$\frac{dn_\ell}{dt} = \frac{n_u}{\tau_{u\ell}} - \frac{n_\ell}{\tau_\ell} + v_g\sigma_0(n_u - n_\ell)N_{ph} \tag{1.40b}$$

$$d_{ap}\frac{dN_{ph}}{dt} = \Gamma v_g\sigma_0(n_u - n_\ell)N_{ph} - \frac{N_{ph}}{\tau_{ph}}d_{ap} \tag{1.40c}$$

It is also convenient to work in terms of photon flux photon flux $\phi_{ph}\left[\frac{1}{\text{area}\times\text{time}}\right]$ instead of photon density $N_{ph}\left[\frac{1}{\text{volume}}\right]$. To convert the system of equations to terms of photon flux, divide by group velocity v_g, approximated as $\frac{c_0}{n_{eff}}$ when ignoring dispersion, so $N_{ph} = \frac{\phi_{ph}}{v_g}$.

$$\frac{1}{v_g}\frac{dn_u}{dt} = \frac{1}{v_g}\eta_{inj}\frac{I}{qV}d_{ap} - \frac{1}{v_g}\frac{n_u}{\tau_u} - v_g\sigma_0(n_u - n_\ell)\phi_{ph} \tag{1.41a}$$

$$\frac{1}{v_g}\frac{dn_\ell}{dt} = \frac{1}{v_g}\frac{n_u}{\tau_{u\ell}} - \frac{1}{v_g}\frac{n_\ell}{\tau_\ell} + v_g\sigma_0(n_u - n_\ell)\phi_{ph} \tag{1.41b}$$

$$d_{ap}\frac{d\phi_{ph}}{dt} = \Gamma v_g\sigma_0(n_u - n_\ell)\phi_{ph} - \frac{\phi_{ph}}{\tau_{ph}}d_{ap} \tag{1.41c}$$

Now simplifying—multiplying through by v_g and d_{ap}—yields our desired set of rate equations.

$$\frac{dn_u}{dt} = \eta_{inj}\frac{J}{q} - \frac{n_u}{\tau_u} - \sigma_0(n_u - n_\ell)\phi_{ph} \tag{1.42a}$$

$$\frac{dn_\ell}{dt} = \frac{n_u}{\tau_{u\ell}} - \frac{n_\ell}{\tau_\ell} + \sigma_0(n_u - n_\ell)\phi_{ph} \tag{1.42b}$$

$$\frac{d\phi_{ph}}{dt} = \Gamma v_g\sigma_0\frac{(n_u - n_\ell)}{d_{ap}}\phi_{ph} - \frac{\phi_{ph}}{\tau_{ph}} \tag{1.42c}$$

1.12 Slope Efficiency

Slope efficiency is the change in output power with current, $\frac{dP}{dI}$. From our rate equations, we have something close to power and current; we have terms of photon flux ϕ_{ph}

and current density J. We can therefore solve for $\frac{d\phi_{ph}}{dJ}$ and convert to slope efficiency

$$\underset{\text{efficiency}}{\text{slope}} = \underset{in}{change} \left(\frac{\text{number of cavity photons}}{\text{pump current}} \right) \times \underset{\text{energy}}{\text{photon}} \times \underset{\text{escape rate}}{\text{photon}}$$

so

$$\frac{dP}{dI} = \frac{d\phi_{ph}}{dJ} \frac{\frac{V_m}{v_g}}{A} \times \mathcal{E}_{ph} \times \frac{1}{\tau_m} \,. \tag{1.43}$$

To solve for $\phi_{ph}(J)$, we can start by solving for the steady state condition of Eq. (1.42c), $\frac{d\phi_{ph}}{dt} = 0$:

$$n_u - n_\ell = \frac{d_{ap}}{\Gamma v_g \sigma_0 \tau_{ph}} \,. \tag{1.44}$$

To find a relation for $n_u - n_\ell$, we solve the steady state conditions for Eqs. (1.42a) and (1.42b), and recover for n_u and n_ℓ, respectively,

$$n_u = \eta_{inj} \frac{J}{q} \frac{\frac{1}{\tau_\ell} + \sigma_0 \phi_{ph}}{\frac{1}{\tau_u}\frac{1}{\tau_\ell} + \sigma_0 \phi_{ph} \left(\frac{1}{\tau_u} + \frac{1}{\tau_\ell} - \frac{1}{\tau_{u\ell}} \right)} \tag{1.45a}$$

$$n_\ell = \eta_{inj} \frac{J}{q} \frac{\frac{1}{\tau_{u\ell}} + \sigma_0 \phi_{ph}}{\frac{1}{\tau_u}\frac{1}{\tau_\ell} + \sigma_0 \phi_{ph} \left(\frac{1}{\tau_u} + \frac{1}{\tau_\ell} - \frac{1}{\tau_{u\ell}} \right)} \tag{1.45b}$$

so that combining Eq. (1.45a) and Eq. (1.45b) yields

$$n_u - n_\ell = \eta_{inj} \frac{J}{q} \frac{\tau_u \left(1 - \frac{\tau_\ell}{\tau_{u\ell}} \right)}{1 + \sigma_0 \phi_{ph} \left(\tau_u \left(1 - \frac{\tau_\ell}{\tau_{u\ell}} \right) + \tau_\ell \right)} = \eta_{inj} \frac{J}{q} \frac{\tau_{eff}}{1 + \sigma_0 \phi_{ph} \left(\tau_{eff} + \tau_\ell \right)} \tag{1.46}$$

using $\tau_{eff} = \tau_u \left(1 - \frac{\tau_\ell}{\tau_{u\ell}} \right)$. Combining the results of Eqs. (1.44) and (1.46) gives

$$\phi_{ph} = \eta_{inj} \frac{J}{q} \frac{v_g \Gamma \tau_{ph}}{d_{ap}} \frac{\tau_{eff}}{\left(\tau_{eff} + \tau_\ell \right)} - \frac{1}{\sigma_0 \left(\tau_{eff} + \tau_\ell \right)} \tag{1.47}$$

and

$$\frac{d\phi_{ph}}{dJ} = \eta_{inj} \frac{v_g \Gamma \tau_{ph}}{q d_{ap}} \frac{\tau_{eff}}{\left(\tau_{eff} + \tau_\ell \right)} \,. \tag{1.48}$$

Again, we have assumed so far only a single QC period. Plugging Eq. (1.48) into Eq. (1.43), we get that the slope efficiency for one period is

$$\frac{dP}{dI} = \eta_{inj} \frac{\mathcal{E}_{ph}}{q} \frac{\alpha_m}{\alpha_m + \alpha_w} \frac{\tau_{eff}}{\left(\tau_{eff} + \tau_\ell\right)} \frac{\int_{x_i}^{x_i + d_{ap}} f^2(x)\, dx}{d_{ap}} \tag{1.49}$$

where the cavity escape and photon lifetimes have been converted to the more common mirror and waveguide loss terms, α_m and α_w $[\frac{1}{\text{length}}]$, such that

$$\frac{1}{\tau_m} = v_g \alpha_m \qquad \text{and} \qquad \frac{1}{\tau_{ph}} = v_g(\alpha_m + \alpha_w)\,. \tag{1.50}$$

We can also introduce here "modal efficiency" Γ_m for period i as

$$\Gamma_{m,i} = \frac{\int_{x_i}^{x_i + d_{ap,i}} f^2(x)\, dx}{d_{ap,i}}\,. \tag{1.51}$$

Summing over all periods, the slope efficiency for the QC laser as a whole is

$$\frac{dP}{dI} = \frac{\mathcal{E}_{ph}}{q} \frac{\alpha_m}{\alpha_m + \alpha_w} \sum_{i=1}^{N_p} \eta_{inj,i} \frac{\tau_{eff,i}}{\left(\tau_{eff,i} + \tau_{\ell,i}\right)} \Gamma_{m,i}\,. \tag{1.52}$$

If all QC periods are the same,

$$\frac{dP}{dI} = N_p \frac{\mathcal{E}_{ph}}{q} \frac{\alpha_m}{\alpha_m + \alpha_w} \frac{\tau_{eff}}{\left(\tau_{eff} + \tau_\ell\right)} \eta_{inj} \Gamma_m\,. \tag{1.53}$$

1.13 Output Power and Wall-plug Efficiency

Having solved for the slope efficiency, a linear relationship for output power results for currents above threshold.

$$P = \frac{dP}{dI}(I - I_{th}) = N_p \frac{\mathcal{E}_{ph}}{q} \frac{\alpha_m}{\alpha_m + \alpha_w} \frac{\tau_{eff}}{\left(\tau_{eff} + \tau_\ell\right)} \eta_{inj} \Gamma_m (I - I_{th}) \tag{1.54}$$

Wall-plug efficiency is simply defined as power out for power in. The input power is simply voltage times current, where the voltage can be broken up into the component

terms representing the photon energy drop $\mathcal{E}_{ph}$, the energy drop Δ_{inj} from the lower laser state of one active region to the upper laser state of the adjacent down-stream active region, and any parasitic series resistance IR_{series}. Thus, input power P_{in} is given by

$$P_{in} = \left(\frac{N_p}{q} (\mathcal{E}_{ph} + \Delta_{inj}) + IR_{series} \right) I \tag{1.55}$$

and the wall-plug efficiency η_{wp} is

$$\eta_{wp} = \left(\frac{\mathcal{E}_{ph}}{\mathcal{E}_{ph} + \Delta_{inj} + \frac{IR_{series}}{N_p}} \right) \left(\frac{\tau_{eff}}{\tau_{eff} + \tau_{\ell}} \right) \left(\frac{\alpha_m}{\alpha_m + \alpha_w} \right) \left(\frac{J - J_{th}}{J} \right) \eta_{inj} \Gamma_m \tag{1.56}$$

expressed as a product of constituent terms, each representing a source of efficiency loss.

1.14 Differential Resistance

$$J = qnv = qn \frac{L_p}{\tau_{trans}} \tag{1.57}$$

$$J = \sigma E \tag{1.58a}$$

$$\sigma = q\mu n \tag{1.58b}$$

$$v = \mu E; J = q\mu nE = qnv = \sigma E \tag{1.58c}$$

$$R = \rho \frac{\ell}{A} = \rho \frac{N_p L_p}{A} \tag{1.58d}$$

$$\sigma = \frac{1}{\rho} = \frac{qnv}{E} = \frac{qnL_p}{\tau_{tr} E} \tag{1.58e}$$

$$R = \frac{N_p L_p}{A} \frac{\tau_{tr}}{qnL_p} E = \frac{N_p L_p}{A} \frac{\tau_{tr}}{qnL_p} \frac{V_{appl}}{N_p L_p} \tag{1.58f}$$

$$R_{active} = \frac{1}{A} \frac{V_{appl}}{qn_{3D} L_p} \tau_{tr} \tag{1.58g}$$

References

[1] I. Vurgaftman, J. R. Meyer, and L. R. Ram-Mohan, "Band parameters for III–V compound semiconductors and their alloys," *J. Appl. Phys.*, vol. 89, no. 11, pp. 5815–5875, 2001. [Online]. Available: http://link.aip.org/link/?JAP/89/5815/1

[2] G. Dehlinger, L. Diehl, U. Gennser, H. Sigg, J. Faist, K. Ensslin, D. Grutzmacher, and E. Muller, "Intersubband Electroluminescence from Silicon-Based Quantum Cascade Structures," *Science*, vol. 290, no. 5500, pp. 2277–2280, 2000. [Online]. Available: http://www.sciencemag.org/cgi/content/abstract/290/5500/2277

[3] O. Malis, L. N. Pfeiffer, K. W. West, A. M. Sergent, and C. Gmachl, "Mid-infrared hole-intersubband electroluminescence in carbon-doped GaAs/AlGaAs quantum cascade structures," *Appl. Phys. Lett.*, vol. 88, no. 8, p. 081117, 2006. [Online]. Available: http://link.aip.org/link/?APL/88/081117/1

[4] S. L. Chuang, *Physics of Optoelectronic Devices*. New York: Wiley, 1995.

[5] G. L. Bir and G. Pikus, *Symmetry and Strain-Induced Effects in Semiconductors*. New York: Wiley, 1974.

[6] C. G. Van de Walle, "Band lineups and deformation potentials in the model-solid theory," *Phys. Rev. B*, vol. 39, no. 3, pp. 1871–1883, Jan 1989.